Journal of Metals, Materials and Minerals, Vol. 29, No. 3, pp. 32-41, 2019

Texture analysis of welded 304L pipeline steel

Soumia HAMZA[1], Zakaria BOUMERZOUG[1*], Anne-Laure HELBERT[2], François BRESSET[2], and Thierry BAUDIN[2]

[1] *Mechanical Engineering Department, LMSM, Biskra University, B.P. 145, Biskra, 0700, Algeria*
[2] *ICMMO, SP2M, Univ Paris-Sud, Université Paris-Saclay, UMR CNRS 8182,91405 Orsay Cedex, France*

[*]**Corresponding author e-mail:** z.boumerzoug@univ-biskra.dz

Received date:
21 January 2019
Revised date:
5 April 2019
Accepted date:
30 June 2019

Keywords:
Stainless steel
Welding
EBSD
Texture
Heat treatments

Abstract

This paper deals with the effect of arc welding process on the crystallographic texture of pipeline 304L steel. The electron backscatter diffraction (EBSD) technique was used to illustrate the effect of welding on the grain orientation in the fusion zone, in the heat affected zone, and in the base metal. Moreover, the effect of isothermal heat treatment at 400°C on welded joint has been studied. The same orientation was found in the base metal and the heat affected zone but different and heterogeneous structures were observed in the fusion zone. The applied heat treatments at 400°C on the welded material had a slight effect on the crystallographic texture, but it had an effect on the grain size in the fusion zone.

1. Introduction

Austenitic stainless steels constitute an important class of engineering materials that have been used widely in a variety of industries and environments due to their high corrosion and oxidation resistance [1-4]. Among the many 300 series austenitic stainless steel grades, AISI 304L stainless steel is extensively used in industries due to its superior low temperature toughness and high corrosion resistance [5].

In the fabrication of equipment made from stainless steels such as pipe, automotive exhaust gas system, chemical industrial equipment, ..., arc welding using shielding gas is often used [6]. Tungsten inert gas (TIG) welding is the most reliable method to weld stainless steels [7]. The welded joint microstructure in any installation can differ significantly from the parent metal. Differences in both welding consumables and the welding process may affect the final weld composition and due to competitive crystal growth which occurs during solidification, preferred crystallographic texture are always observed [8]. Heat generated during welding induces an important temperature gradient in and around the welded area or fusion zone (FZ). The microstructure that develops in the FZ varies noticeably from region to region. The zone outside the fusion zone that is thermally affected by the welding treatment is known as the heat-affected zone (HAZ) [9]. In addition, the understanding of the grain structure development in the FZ of polycrystalline welds is limited. This is because many competitive transformations have been observed.

However, the most previous works on welding of 304L stainless steel were focused on microstructure and corrosion behavior of welded material [1,10-13] and a limited published works were devoted to the texture investigation in welded 304L stainless steel [14]. EBSD analysis of the as-welded specimens revealed that the primary solidification occurred in <101> direction and grain growth occurred in either <001> or <111> direction depending on the variable welding parameters [14]. In our previous work [15], we found that the texture was affected by the welding process of an industrial low carbon steel. In this welded steel, HAZ contains grains larger than those in the base metal and tend to grow along a certain preferred crystallographic direction.

Furthermore, investigating and controlling texture are necessary because it affects mechanical properties. In this context, the aim of the present work is to investigate the crystallographic texture in welded 304L stainless steel and also to study the heat treatment effect on the crystallographic texture which has not been studied before. The importance of this study lies in the use of this type of steel to transport a natural gas. Consequently, understanding the microstructure in welded joint is crucial for high quality of the welding process.

2. Experimental

In this study, the base metal (BM) was AISI 304L austenitic stainless steel used for transport gas pipeline applications. Table 1 presents the chemical composition of the AISI 304L which has been determined by the EDS technique.

To meet strength and safety requirements and to produce good quality welds, V-shaped butt welds were prepared using two consecutive passes with gas tungsten arc welding (GTAW) method and ER-308L filler was used as electrode. The welding process performed with speed of 6 $cm \cdot min^{-1}$, where the inputs were 22 V and 90 A. The chemical composition of the electrode is presented in Table 2.

DOI: 10.14456/jmmm.2019.31

Table 1. Chemical composition of the base metal (wt.%).

Fe	C	Mn	Si	P	S	Ni	Cr
Balance	0.026	1 .07	0.40	0.038	0.001	8.11	18.50

Table 2. Chemical composition of the base metal (wt.%).

Fe	C	Mn	Si	P	S	Ni	Cr
Balance	0.026	1 .07	0.40	0.038	0.001	8.11	18.50

To avoid a penetration into weld region of some undesirable elements (N_2, O_2, H_2), argon gas was used during welding with flow rate 15 $l \cdot min^{-1}$. Figure 1 presents the schematic illustration of a butt weld specimen. After welding, a transverse cross section (perpendicular to the welding direction) of samples was cut for EBSD analyses.

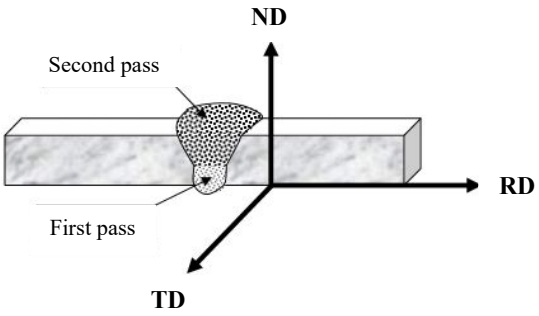

Figure 1. Schematic illustration of the butt weld specimen with the sheet coordinate system: Rolling Direction (RD), Transverse Direction (TD) and Normal Direction (ND).

In order to study the heat treatment effect on welded specimens, an isothermal annealing was performed in electrical furnace at 400°C during 30 min. Then, detailed texture, *grain size and morphology studies* were carried out in the FZ, HAZ, and BM region. EBSD specimens were prepared in the standard manner (mechanical polishing with SiC paper and electro polishing with the A2 Struers solution during 12 s in 40V flux 12). EBSD measurements were performed on the sample transverse cross section using a Scanning Electron Microscope (SEM) with a Field Emission Gun (FEG) SUPRA 55 VP operated at 20 kV with a TSL orientation imaging system (using OIM™ software). EBSD maps covered sample area of about 7 mm x 7 mm of cross-section of the weld joint (on the transverse plane perpendicular to the weld direction) (Figure 2) with a step size of 2 µm. To study at least half of the welded joint by the EBSD technique, 20 maps of welded material, and 27 maps of welded and heat treated at 400 °C have been studied.

The pole figures and the orientation distribution function (ODF) are calculated, using the harmonic series expansion (rank L = 22) method, from the orientations measured by EBSD. Each orientation is modeled by Gaussian function with a 5° half width. Even if the EBSD maps are measured in the (ND, RD) plane, the crystallographic orientation is described in the (RD, TD) sheet rolling plane.

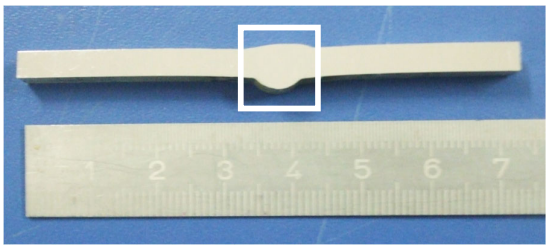

Figure 2. Macrographic view of welded 304L steel. The red square indicates approximately the analyzed area by EBSD.

3. Results and discussion

3.1. Texture in welded joint

Figure 3 shows EBSD map of the half part of the welded joint of 304L stainless steel which contains the BM, HAZ and the half part of FZ. The color of individual grains describes the {hkl} crystallographic plane parallel to the observation plane. This EBSD map gives a general idea about the grain morphology and orientation in each zone. The microstructure of either BM or HAZ is characterized by finer equiaxed-grains, however the FZ adjacent to the HAZ is totally different from other zones (HAZ, BM), and composed of different sub-zones with different grain morphologies.

3.1.1 The texture of the base metal

It is well known that the microstructure of austenitic stainless steel is mainly composed of austenite under the condition of equilibrium solidification. Concerning the texture of the BM, its EBSD map indicates a polygonal shape of the grains (Figure 4a). On the basis of three poles figures of planes {001}, {011} and {111} (Figure 4b) and the ODF (Figure 4c), the texture of the base metal corresponds to the major {110} <001> Goss texture. The minor near {110} <111> orientation is also observed (Figures 4b and 4c).

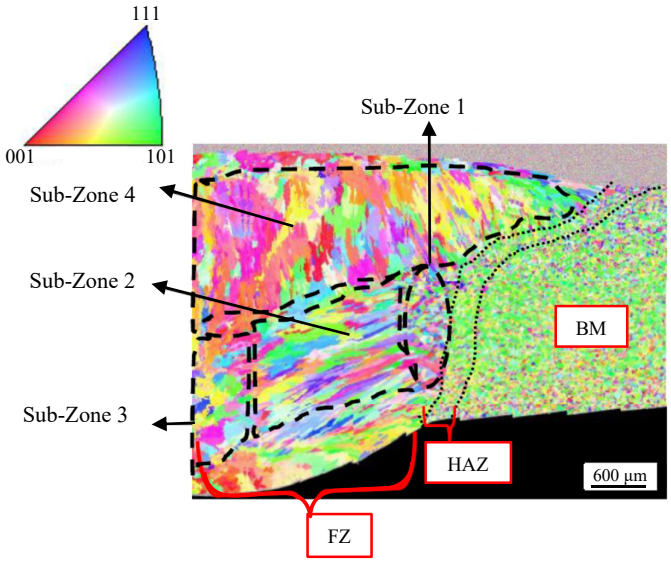

Figure 3. EBSD map of BM, HAZ and FZ (with selected sub-zones 1, 2, 3 and 4) in welded 304L stainless steel. The color code is given on the standard triangle. (First pass contains three sub-zones 1, 2 and 3. Second pass contains sub-zone 4)

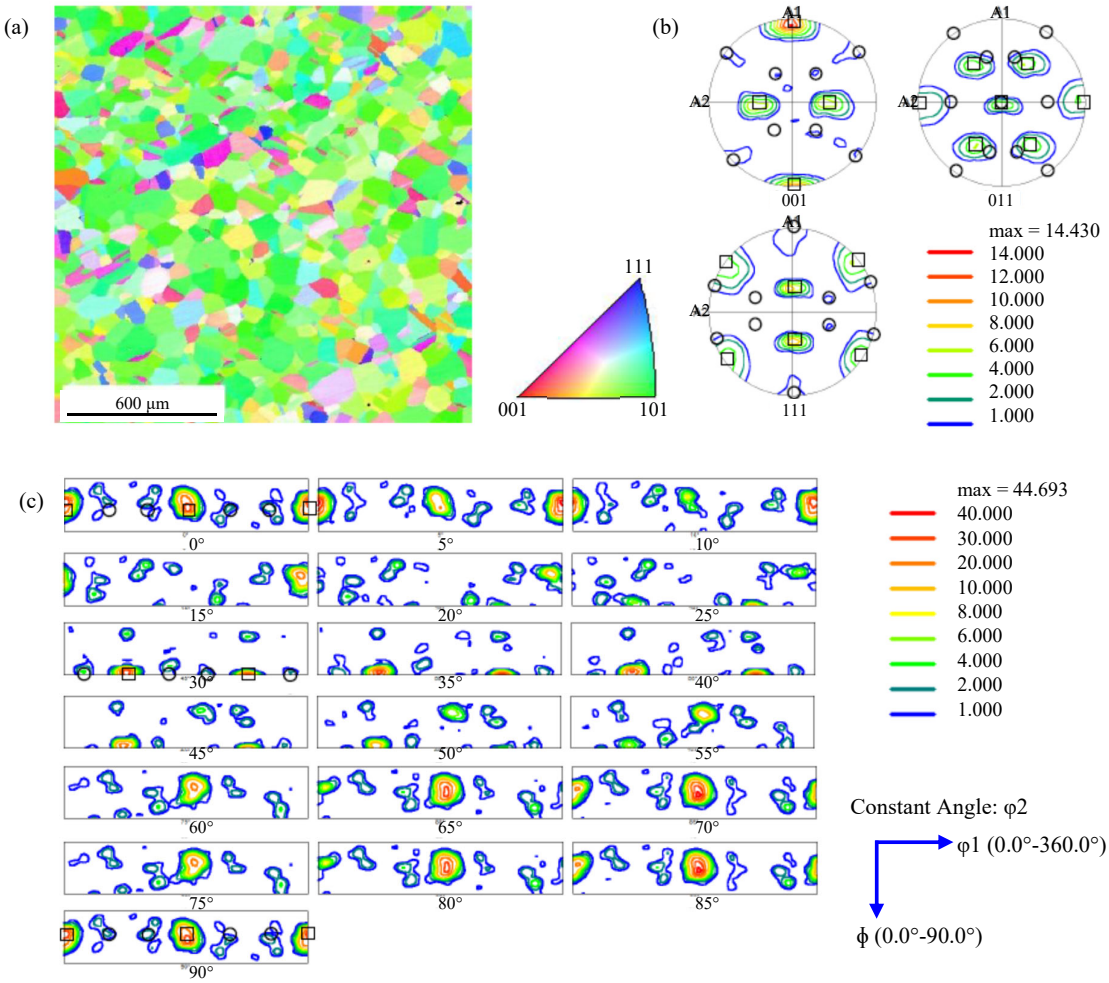

Figure 4. (a) EBSD map (step size = 0.5 µm), (b) {001}, {011} and {111} pole figures, and (c) ODF of BM in the welded 304L stainless steel. (□ Goss orientation and ○ {110}<111> orientation).

3.1.2 The texture of the heat affected zone

The HAZ is a narrow zone and it represents a transition zone between FZ and the base metal. HAZ is generally composed of an austenite matrix and interspersed ferrite precipitates, because, during the non-equilibrium rapid solidification conditions, such as in welding, the high cooling rate will result in incomplete $\gamma \rightarrow \delta$ transformation and small amounts of δ-ferrite should be remained unavoidably in the weld microstructure at room temperature. The retained δ-ferrite is known to prevent solidification and hot cracking and to improve ductility, toughness and corrosion resistance. However, it is also reported that excess δ-ferrite (usually more than 10 vol%) can decrease the hot workability [16].

As presented in Figure 5, the texture of HAZ corresponds to the {110} <001> Goss orientation. The minor near {110} <111> orientation is still present such as in the BM. In this zone, the texture acuity is slightly lower than in BM. This difference is probably due to the effect of heat input during welding process.

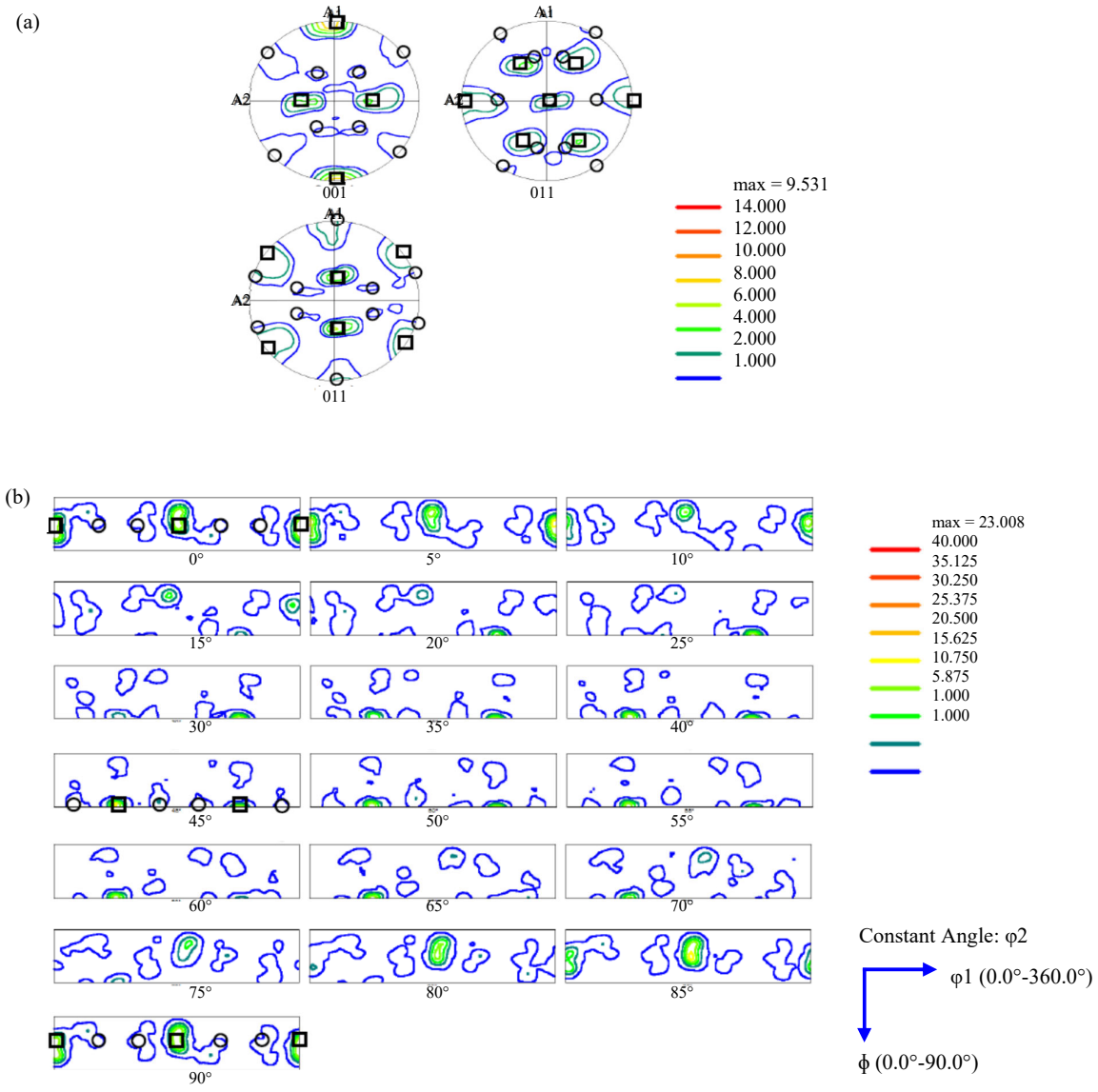

Figure 5. (a) {001}, {011} and {111} pole figures and (b) ODF of HAZ in the welded 304L stainless steel. (□ Goss orientation and ○ {110}<111> orientation).

3.1.3 The texture of the fusion zone

Concerning the microstructure of FZ, the majority of the grains in fusion zone have columnar structure with preferred directions. During growth of the solid in the weld pool, the shape of the solid-liquid interface controls the development of microstructural features [17]. This columnar microstructure is due to the preferred mechanism of solidification after welding process which has been observed in previous works [18-20].

For clarity, four distinct sub-zones were considered in FZ (sub-zones 1, 2, 3, and 4). The texture of FZ varies according the sub-zones. The difference of the microstructure inside the FZ is due to the difference of cooling rates which were caused by the heat flow during welding process. For example, the microstructure of sub-zone 1 exhibits an *isotropic* polycrystalline structure (Figure 6). In general, development of equiaxed grain structure induces best mechanical properties of weld.

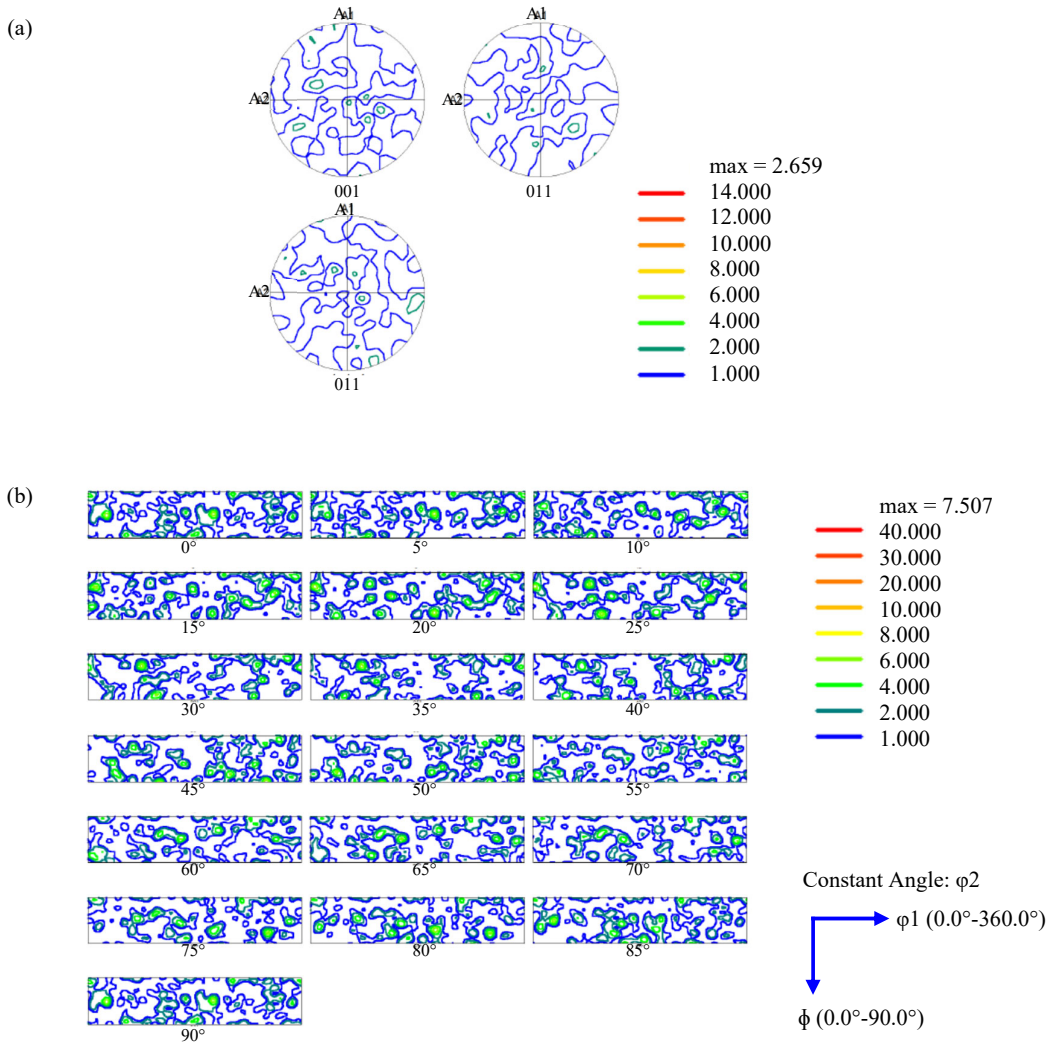

Figure 6. (a) {001}, {011} and {111} pole figures and (b) Orientation Density Function (ODF) of fusion zone, sub-zone 1 in the welded 304L stainless steel.

Finally, the sub-zone 4 exhibits a partial {100} <uvw> fiber that is slightly rotated around ND (A1). In this fiber, the Cube component is preferentially developed (Figure 9). These oriented grains form as extensions of grains of sub-zone 3. This sub-zone texture corresponds to the solidification growth direction after the second pass of welding because the austenitic grains grow with a coarse columnar structure along the preferential growth direction. Let us note that such coarse columnar structure is susceptible to hot cracking [27].

For brevity, Table 3 presents the crystallographic texture on the BM, HAZ, and FZ in welded 304L stainless steel.

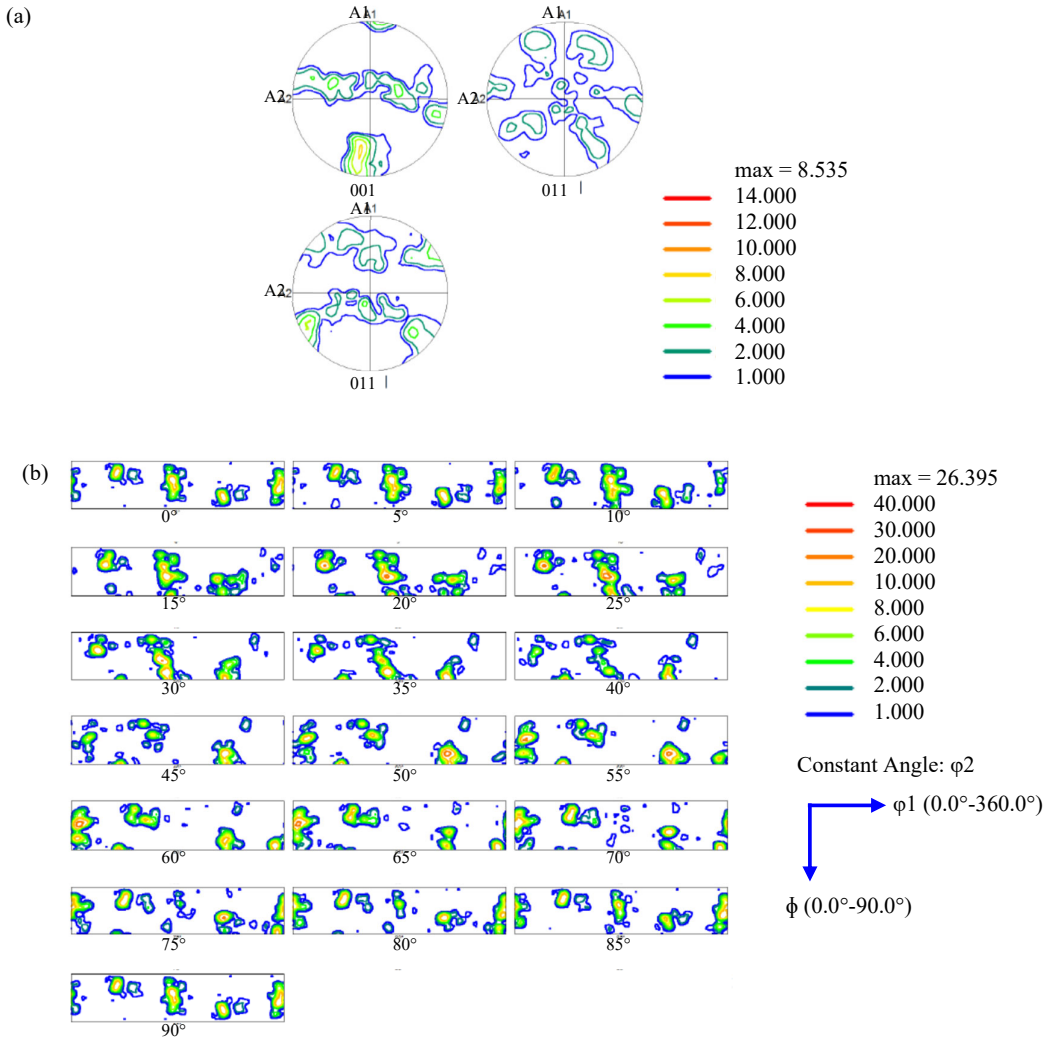

Figure 7. (a) {001}, {011} and {111} pole figures and (b) ODF of FZ sub-zone 2 in the welded 304L stainless steel.

It is convenient to consider the FZ as a mini-casting and fundamental solidification mechanisms developed primarily for cast metals have been successfully applied to the welds [26-27]. Based on the developed structures in fusion zone of welded 304L stainless steel and above considerations, a schematic illustration of solidification mechanism is proposed (Figure 10). Therefore, the microstructures formed in FZ of welded 304L stainless steel contain three successive main sub-zones. First, a sub-zone formed by finer grains, adjacent to the HAZ is followed by large columnar grains and stopped by an equiaxed grains area formed in third sub-zone. This grain distribution is identical to the grain distribution in steel ingots because most castings have three zones: the chill zone, columnar zone, and equiaxed zone [28]. The chill zone corresponds to the finer grain zone which is due to the rapid nucleation that occurs because the molten metal comes into contact with the base metal.

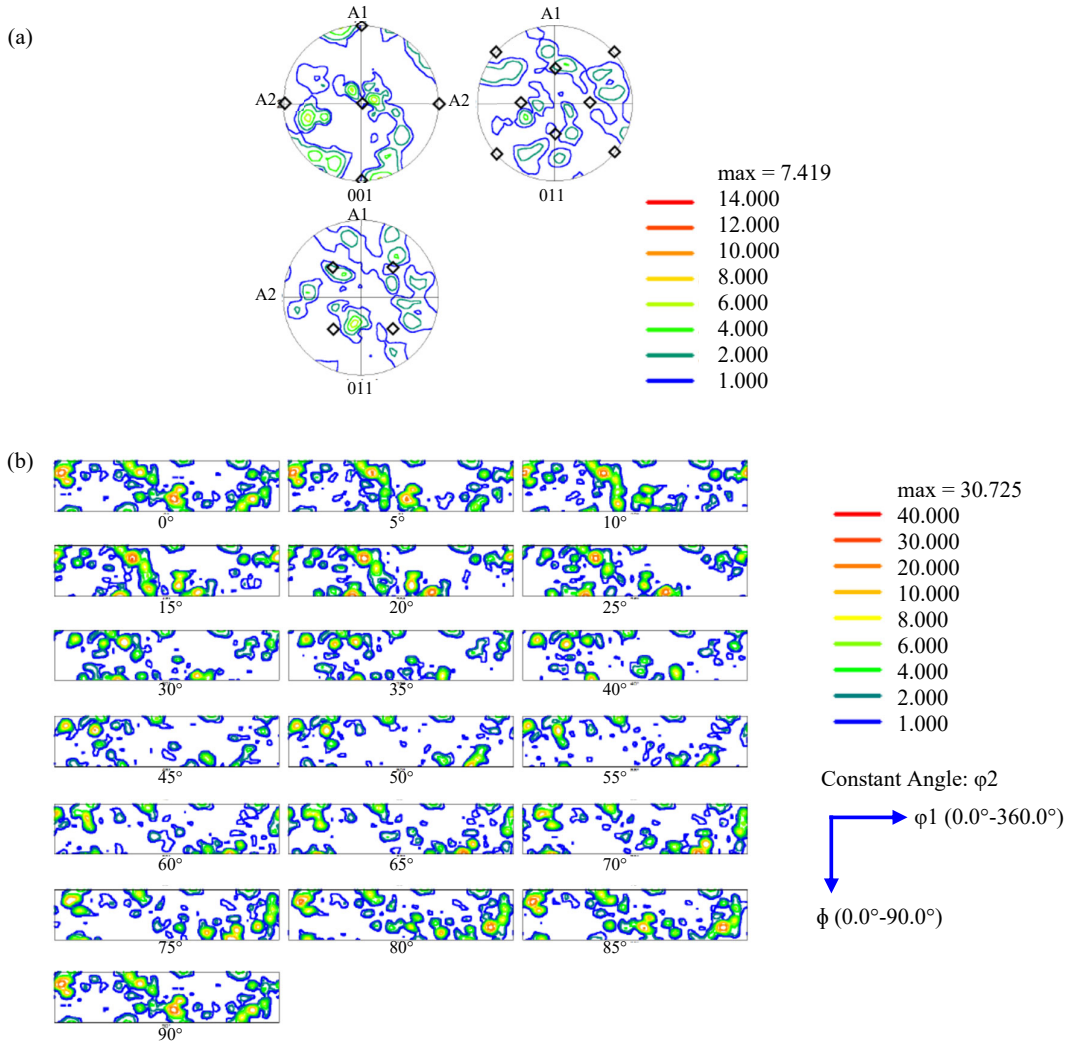

Figure 8. (a) {001}, {011} and {111} pole figures and b) ODF of FZ sub-zone 3 in the welded 304L stainless steel. (◊ {100}<001> Cube orientation).

Based on the present results, it is necessary to mention that the welded joint is characterized by some textures which have not been mentioned by Ha et al. [29]. These authors found that the heat input during welding process of 304 stainless steel, produces a random texture.

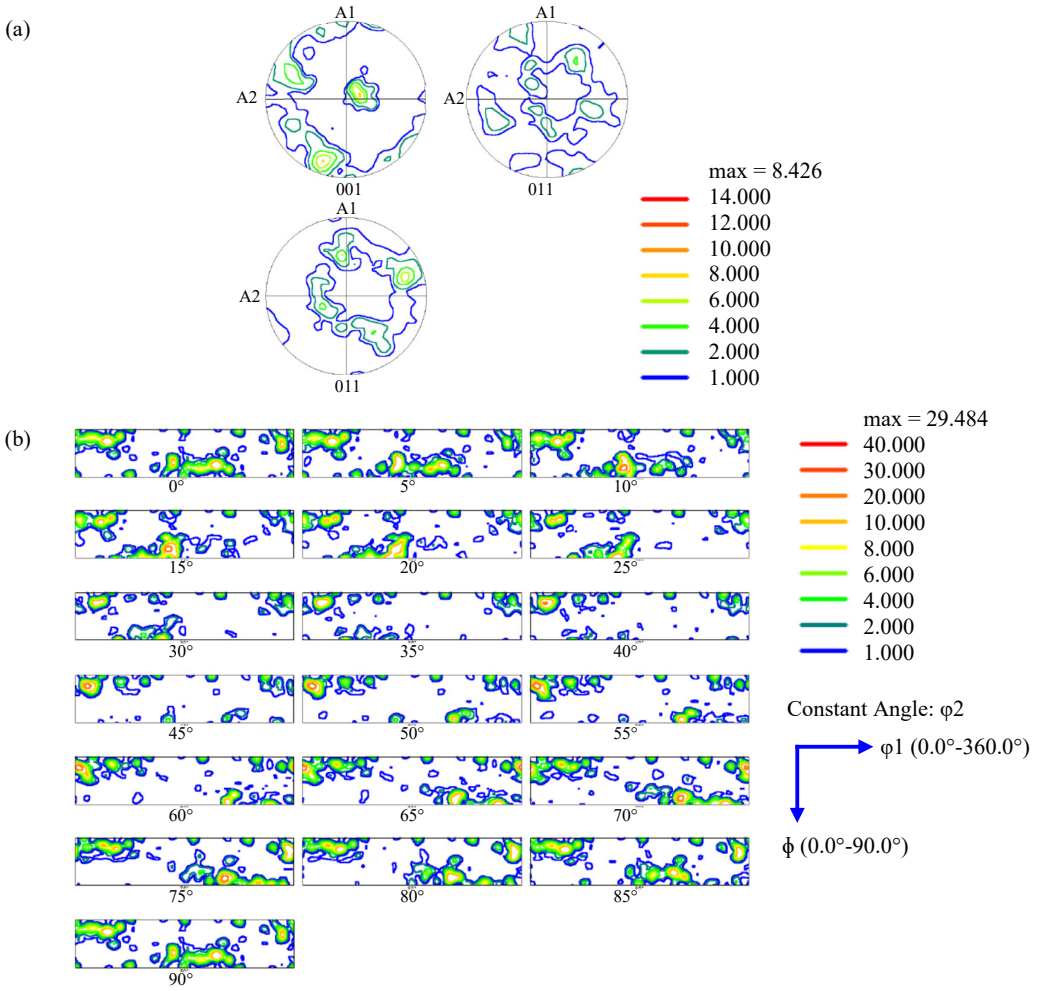

Figure 9. (a) {001}, {011} and {111} pole figures and (b) ODF of FZ sub-zone 4 in the welded 304L stainless steel.

Table 3. Microstructure and textures in BM, HAZ and FZ of welded 304L stainless steel.

	BM and HAZ	FZ
Microstructure	Equiaxe grains	Sub-zone 1: Equiaxe grains Sub-zone 2: columnar grains Sub-zone 3: Equiaxe grains Sub-zone 4: columnar grains
Texture	Major {110}<001> Goss component with minor orientation close to {110}<111>	Sub-zone 1: *Isotropic texture* Sub-zone 2: Fiber close to {hkl}<001> Sub-zone 3: Near {100}<001> Cube orientation plus other not ideal orientations Sub-zone 4: Fiber close to {100}<uvw> with a major Cube component

3.2 Effect of heat treatment on texture evolution in welded join

Figure 11 presents a general view of the welded joint (EBSD maps) after heat treatment at 400°C during 30 minutes of welded 304L stainless steel. The finer grains observed in sub-zone 1 of the unheated welded steel disappear inside the FZ, i.e., there was a grain growth reaction during this isothermal annealing**.**

Except the disappearance of the sub-zone 1, the heat treatment does not modify the microstructure and the texture of the weld.

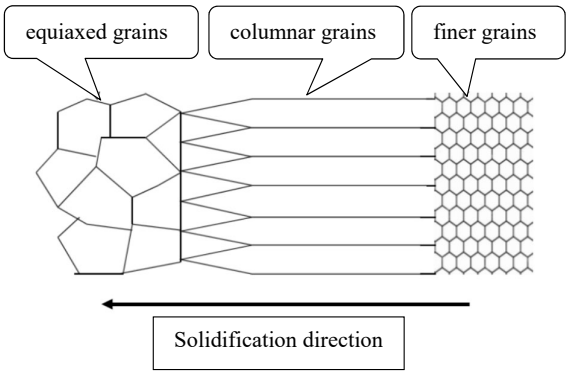

Figure 10. Schematic illustration of solidification mechanisms in FZ of welded 304L stainless steel.

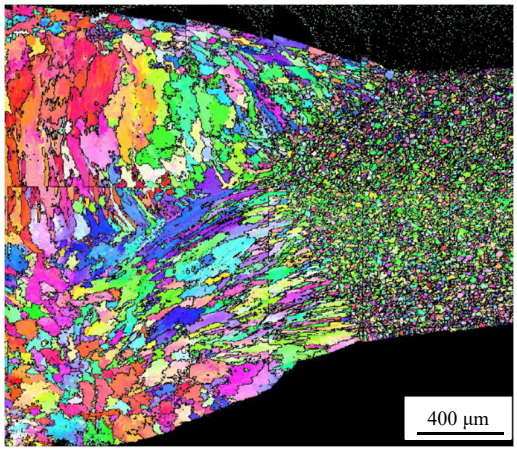

Figure 11. EBSD maps after heat treatment at 400°C during 30 minutes of welded 304L stainless steel.

4. Conclusions

The investigation by the EBSD technique of welded of AISI 304L stainless steel has showed different grain morphologies and textures. In summary, three distinct zones were observed in the welded joint which are the base metal, the heat affected zone and the fusion zone. However, our present findings give more details about the texture in the different zones and more particularly in the FZ. The texture in welded 304L stainless steel is not random. The main conclusions can be drawn:

- The BM presents an equiaxe grain structure and its texture is composed of a major Goss orientation and minor component close to {110} <111>.
- In the HAZ, the microstructure and the texture are similar to those observed in the BM.
- The microstructure and the texture in FZ depend on each selected sub-zone inside this region. However, the main zones are described by a columnar microstructure and a <100> or {100} fiber for the first and the second pass of welding, respectively. In the first join, two areas of equiaxe grains are found. The first one, with finer grains is isotropic and situated near the HAZ. The second one, in the middle of the weld, shows a near Cube orientation with a large spread plus some other orientations not easily identifiable.

The isothermal heat treatment (30 min at 400°C) leads to the disappearance of the finer grains in the FZ, but the texture was not affected.

References

[1] G. R. Mirshekari, E. Tavakoli, M. Atapour, and B. Sadeghian, "Microstructure and corrosion behavior of multipass gas tungsten arc welded 304L stainless steel," *Materials and Design*, vol. 55, pp. 905-911, 2014.

[2] J. Wang, J. Xionga, Q. Pengb, H. Fana, Y. Wang, G. Lia, and B. Shen, "Effects of DC plasma nitriding parameters on microstructure and properties of 304L stainless steel," *Materials Charact*erization, vol. 60, pp. 197-203, 2009.

[3] G. Kiymaz and E. Seckin, "Behavior and design of stainless steel tubular member welded end connections," *Steel and Composite Structures*, vol.17, 3, pp. 253-269, 2014.

[4] X. Chen, G. Chen, and D. Li, "Ratcheting behavior of pressurized Z2CND18.12N stainless steel pipe under different control modes," *Steel and Composite Structures*, vol.18, pp. 29-50, 2015.

[5] W. F. Smith, *Structure and properties of engineering alloys.* 2nd ed. New York: McGraw-Hill, 1993.

[6] G. Lothongkum, E. Viyanit, and P. Bhandhubanyong, "Study on the effects of pulsed TIG welding parameters on delta-ferrite content, shape factor and bead quality in orbital welding of AISI316l stainless steel plate," *Journal of Materials Processing Technology*, vol. 110, pp. 233-238, 2001.

[7] A. Gholipour, M. Shamanian, and F. Ashrafizadeh, "Microstructure and wear behavior of stellite 6 cladding on 17–4 PH stainless steel," *Journal of Alloys and Compounds*, vol. 509, 14, pp. 4905-4909, 2011.

[8] J. Sule, S. Ganguly, H. Coules, and T. Pirling, "Application of local mechanical tensioning and laser processing to refine microstructure and modify residual stress state of a multi-pass 304L austenitic steels welds," *Journal of Manufacturing Processes*, vol. 18, pp. 141-150, 2015.

[9] A. Mostafa and S. Bordbar, "Applying a novel heat treatment cycle to modify the microstructure of welded APIX70 pipeline steel," *Materials Letters*, vol. 98, pp.178-181, 2013.

[10] C. M. Lin, H. L. Tsai, C. D. Cheng, and C. Yang, "Effect of repeated weld-repairs on microstructure, texture, impact properties and corrosion properties of ISI 304L stainless steel," *Engineering Failure Analysis*, vol. 21, pp. 9-20, 2012.

[11] P. K. Giridharan and N. Murugan, "Optimization of pulsed GTA welding process parameters for the welding of 304L stainless steel sheets," *The International Journal of Advanced Manufacturing Technology* , vol. 40, pp. 478-489, 2009.

[12] S. A. A., Akbari Mousavi and R. Miresmaeili, "Experimental and numerical analyses of residual stress of distributions in TIG welding process for 304L stainless steel," *Journal of Materials Processing Technology* , vol. 208, pp. 383-394, 2008.

[13] Z. Boumerzoug, S. Hamza and, V. Ji, "Effect of heat treatment on the microstructural evolution in weld Region of 304l pipeline steel," *Journal of Thermal Engineering*, vol. 2, pp. 1017-1022, 2016.

[14] S. Saha, M. Mukherjee, and T. K. Pal, "Microstructure, texture and mechanical property analysis of gas metal arc welded AISI304 austenitic stainless steel," *Journal of Materials Engineering*, vol. 24, pp. 1125-1139, 2015.

[15] Z. Boumerzoug, C. Derfouf, and T. Baudin, "Effect of welding on microstructure and mechanical properties of an industrial low carbon steel," *Engineering*, vol. 2, pp. 502-506, 2010.

[16] H. Mecking, *Preferred orientation in deformed metals and rocks: An introduction to modern texture analysis*, California, Ed. Hans Rudolf Wenk, 1985.

[17] S. A. David, S. S. Babu, and J. M. Vitek, "Welding: Solidification and microstructure," *JOM,* vol. 55 pp. 14-20, 2003.

[18] A. F. Norman, I. Brough, and P. B. Prangnell, "High resolution EBSD analysis of the grain structure in an AA2024 friction stir weld," Proceeding of the 7th International conference on Aluminium Alloys (ICAA-7), Virginia, Trans Tech Publications, USA, pp. 1713-1718, 2000.

[19] K. Tagashira, K. Kikuchi, and T. Tanaka, "Solidification texture in aluminum beads welded using a CO_2 laser," *Journal of the Japan Institute of Metals*, vol. 64, pp. 407-412, 2000.

[20] S. Babu, H. K. D. H. Bhadeshia, and L. E. Svenson, "Crystallographic texture and the austenite grain structure of low-alloy steel weld deposits," *Journal of Materials Science Lett*ers, vol. 10, pp. 142-144, 1991.

[21] Course "Solidification of Weld Metal" (2013) Available from: http://nptel.ac.in/courses/112107090/33

[22] A. O. Kluken, Ø. Grong, and J. Hjelen, "The origin of transformation textures in steel weld metals containing acicular ferrite," *Metallurgical Transactions A*, vol. 22, pp. 657-663, 1991.

[23] Ø. Grong and D. K. Matlock, "Microstructural development in mild and low –alloy steel weld metals," *International Metals Reviews*, vol. 31, pp. 27-48, 1986.

[24] A. O. Kluken, Ø. Grong, and G. Rorvik, "Solidification microstructures and phase transformations in Al-Ti-Si-Mn deoxidized steel weld metals," *Metallurgical Transactions A*, vol. 21, pp. 2047-2058, 1990.

[25] H. L. Wei, J. Mazumder, and T. DebRoy, "Evolution of solidification texture during additive manufacturing," *Scientific Reports 5*, Article number: 16446, 2015.

[26] A. A. Ugla, "Enhancement of weld quality of AISI 304L austenitic stainless steel using a direct current pulsed TIG arc," presented at 2nd International Conference on Engineering Sciences. IOP Conference Series: Materials Science and Engineering, Kerbala, Iraq, 2018.

[27] S. David and J. Vitek, *International trends in welding science and technology*, ASM, 1993.

[28] F. C. Campbell, *Elements of metallurgy and engineering alloys*. Ohio: ASM International, 2008.

[29] X. H. Ha, S. W. Jang, W. H. Bang, U. S. Yoon, and K. H. Oh, "Texture, Evolution in Weld Regions of SUS-304 Stainless Steel and TRIP Steel," *Materials Science Forum*, vol. 408-412, pp. 1377-1382, 2002.